

Article

Direct and Indirect Evidence of the Microbially Induced Pitting Corrosion of Steel Structures in Humid Environments

Jingzhong Zhou ¹, Kuoteng Sun ¹, Songqiang Huang ¹, Xuemin He ¹, Zhaowei Hu ^{2,*} and Wenge Li ^{2,*}

¹ Liuzhou Bureau of EHV Transmission Company, China Southern Power Grid Co., Ltd., Liuzhou 545006, China; zjzking@163.com (J.Z.); sunkuoteng@163.com (K.S.); foobarx@163.com (S.H.); hexuemin012@163.com (X.H.)

² Merchant Marine College, Shanghai Maritime University, Shanghai 201306, China

* Correspondence: huzw@shmtu.edu.cn (Z.H.); wgli@shmtu.edu.cn (W.L.)

Received: 9 September 2020; Accepted: 13 October 2020; Published: 15 October 2020



Abstract: Corrosion is a severe problem for steel structures in humid environments. In particular, humidity usually triggers the surface adhesion of microorganisms, leading to microbiologically induced corrosion. This study aims to explore the effect of bacterial biofilm formation on the pitting corrosion of stainless steel. This research uses electrochemical methods to obtain indirect evidence of the pitting corrosion of steel. In addition, in order to obtain direct evidence of the pitting corrosion of stainless steel, field emission scanning electron microscopy (FESEM) and atomic force microscopy (AFM) were used to characterize the dimensional morphology of the stainless steel after pitting. It was shown that the bacterial adhesion increased with the pH and temperature, which significantly increased the surface roughness of the stainless steel. Electrochemical analysis revealed that the formation of biofilm greatly destroyed the oxide film of 304 SS and accelerated the corrosion of stainless steel by forming an oxygen concentration battery. SEM and AFM analyses showed cracks and dislocations on the surface of stainless steel underneath the attached bacteria, which suggested a direct role of biofilm in corrosion induction. The results presented here show that the bacterial biofilm formation on the steel surfaces significantly accelerated the corrosion and affected the pitting corrosion process of the steel structure.

Keywords: microbiologically induced corrosion; pitting corrosion; electrochemical testing; steel structure; SEM; AFM

1. Introduction

Corrosion has long been a major concern for steel structures. In some harsh environments—for instance, in humid service environments—microorganisms attach easily to steel surfaces and develop highly organized communities known as biofilms [1–3]. Humidity has been one of the major concerns for the maintenance of steel-structured high-voltage transmission line towers in southern China. Biofilm formation is a multi-stage process, with the adhesion of microorganisms such as bacteria as one of the most important steps [4]. Depending upon where they grow, these bacteria can be beneficial to wastewater treatment [5] or troublesome in biomaterial-related infections [6] and engineering equipment fouling and corrosion [7]. In humid environments, the attachment of bacteria will significantly affect the corrosion of materials [8,9], and pitting corrosion is one of the main means of damage [10]. It is not surprising that microbiological effects are of significant concern in failure analysis and prevention. Microbially induced corrosion problems afflict water-handling operations and manufacturing processes in oil and gas production, pipelining, refining, petrochemical synthesis,

power production, fermentation, waste water treatment, drinking water supply, pulp and paper making, and other industrial sectors. Microbially induced corrosion is also a concern whenever metals are exposed directly to the environment in applications including marine or buried piping, storage tanks, ships, nuclear waste containers, pilings, marine platforms, and so on.

Many studies have reported the effects of bacterial attachment on the pitting corrosion of metallic materials in humid environments [11,12]. The causes of pitting corrosion can be divided into four categories: physical factors, chemical factors, biological factors, and metallurgical factors [13]. Corrosive ions such as Cl^- and organisms act as chemical and biological factors for the pitting corrosion of metallic materials. Especially for steels [14], their physical and chemical properties are severely affected by fouling organisms attached to their surfaces [15,16]. The role of bacteria in the pitting corrosion of steels has been a concern of researchers. Yin et al. [17] studied the possible mechanism of accelerated pitting corrosion in 303 stainless steel by *Vibrio natriegens*. It was found that the fixation of nitrogen by this bacterium promoted the pitting corrosion of 303 stainless steel, where the effect of ammonia was negligible. Xu et al. [18] investigated the role of *Pseudomonas aeruginosa* in the pitting process of 2205 duplex stainless steel. Their results showed that *Pseudomonas aeruginosa* produced soluble CrO_3 on the surface of the duplex stainless steel, which accelerated the dissolution of the passivation film, in turn contributing to pitting corrosion. Moreover, simulation models were also proposed to study crucial factors affecting the corrosion process [19]. However, there is still a lack of knowledge on the mechanisms of the pitting process by fouling microorganisms on steel.

Electrochemical methods have been widely used as an indirect measurement technique to study pitting corrosion. For example, Igual Muñoz et al. [20] studied the effect of bromide concentration and the presence of chromate in solution on the pitting behavior of 2205 duplex stainless steel using cyclic polarization curves and impedance measurements. Their results showed that the pitting potential increased with the increase in the lithium bromide concentration in a semi-logarithmic decreasing trend, suggesting that the addition of bromide reduced the pitting corrosion ability of the chromate on the stainless steel. While electrochemical studies can be used to investigate pitting corrosion, these approaches cannot be used to study and identify microscale pit features [21]. Recently, scanning electron microscopy (SEM) has been used to characterize the morphology of single pits and the growth of pits based on the corrosion morphology. Zhu et al. [22] investigated the influence of additives on the pitting process of 2024-T3 aluminum alloy in a neutral sodium chloride solution using SEM. It was found that bis-[3-(triethoxysilyl) Propyl] tetrasulfide inhibited the pitting corrosion of the aluminum alloy. Pidaparti et al. [23] studied the pitting/cracking of nickel-aluminum bronze alloy in a composite corrosive environment comprised of ammonia and artificial seawater. More recently, AFM observation was used to study the characteristic features of the pitting process. Pan et al. [24] conducted an in situ AFM observation of the pitting corrosion behavior of 304 stainless steel and its nanocrystallization thin films in 3.5% NaCl solution, indicating that nanocrystallization changed the geometry and growth mechanism of stable pits. Zhang et al. [25] investigated the pitting corrosion behavior of 304 stainless steel in 3.5% NaCl solution with the in situ AFM method. The results showed that pitting corrosion products played a major role in promoting the growth of pits. Yet, there are limited studies of pitting corrosion that utilize a combined method of electrochemical testing and direct observation (including SEM and AFM) [26,27].

Pitting corrosion is a long process for stainless steel in humid environments, however most researchers have focused on the effect of microorganisms on the pitting of materials within 30 days [8,9,28]. Long-term data of the high-voltage transmission line tower caused by the microbiologically induced corrosion is yet lacking. In this study, we investigated the effects of different environmental factors—including pH, temperature, and culture age (90 days)—which directly affect the extent of the initial adhesion of typical bacteria and bacterial biofilm formation. The indirect evidence of the effect of *Bacillus sp.* biofilm formation on the pitting of the steel was analyzed using an electrochemical method. Moreover, the pitting morphology of the steel surfaces was observed

through SEM and AFM images to provide direct evidence of the impact of bacterial biofilm on the pitting corrosion.

2. Materials and Methods

A typical bacteria *Bacillus sp.* strain (MCCC1A00791) was used in this study. The culture medium for the *Bacillus sp.* was prepared by dissolving 1 g of yeast extract and 5 g of peptone in 1000 mL of artificial sea water (ASW), which modelled the typical humid environments in most places of southern China close to the sea. The bacteria suspension was shaken at 30 °C for 24 h. The inoculated medium of *Bacillus sp.* was prepared with a density of 10^6 cells/mL by dilution at 30 °C under aerobic conditions.

304 stainless steel (304 SS) plates (10 mm × 10 mm × 2 mm) were typically used as the substrates in this study. The substrates were polished to a mirror finish, followed by a brief rinsing with distilled water, and cleaning ultrasonically in acetone. Prior to performing the corrosion testing, the samples were sterilized with 75% ethanol and UV light for 1 h. All the tests were carried out in ASW. Peptone at 3.0 g/L was added to ASW as carbon and energy sources for the bacteria and sterilized at 121 °C for 20 min. The culture media were refreshed every 2 days. To investigate the effect of pH on the bacterial attachment, the media were adjusted to a pH of 4.5, 7, and 9. In order to study the effect of the culture temperature, the inoculated media was grown at 4, 20, and 30 °C.

A field emission scanning electron microscope (FESEM, FEI Quanta FEG 250, Amsterdam, The Netherlands) was used to characterize the morphology of the surface of the 304 SS specimens and identify any unique features that appeared after exposure to the bacterial media. The energy of the accelerator beam used was 5 kV. A confocal laser scanning microscope (CLSM) (Leica TCS SP5 II, Wetzlar, Germany) was utilized to observe the bacterial attachment and obtain images of the biofilm on the 304 SS surfaces. After incubation, the samples were rinsed with distilled water three times to remove the bacteria that did not adhere to the samples, which was followed by fixation in 2.5% glutaraldehyde. Then, the samples were stained with 150 µL of propidium iodide (PI) for 30 min in the dark, followed by three cycles of cleaning with PBS. The Z-stack technique was used to measure the thickness of the biofilm. A Zeiss LSM 700 confocal laser scanning microscope was used to observe the surface topography of the steel samples before and after their immersion in ASW media. To analyze the biofilm and the pits that formed on the surface, AFM (Dimension™ 3100, Digital Instrument Inc., Veeco, Santa Barbara, CA, USA) in air was used in tapping mode (RTESP Silica cantilever, spring constant: 40 N/m). To examine the extent of the biocorrosion of 304 SS, the biofilm on the substrate was removed by ultrasonic cleaning with distilled water for 5 min and with 17% nitric acid for 2 min, followed by rinsing with distilled water.

Electrochemical testing was conducted in a three-electrode cell system where a platinum plate and a saturated calomel electrode (SCE) were used as the counter electrode and reference electrode, respectively [28]. The samples with an exposed area of 1 cm² served as the working electrode. The steel samples were immersed in clean ASW and also in ASW that contained bacteria, and incubated at 30 °C in a shaker at 120 rpm. Cyclic potentiodynamic polarization (CPP) and electrochemical impedance spectroscopy (EIS) spectra were obtained by a Solartron Modulab system (2100A, Solartron Electronic Group, Leicester, UK). EIS measurements were achieved by applying an AC signal of 10 mV at a frequency ranging from 100 kHz to 0.01 Hz. The obtained data were then analyzed using ZSimpWin (version 3.30). The CPP curves were acquired by scanning the potential in the forward direction with a scanning rate of 0.5 mV/s from −500 to 900 mV. For the back scan, the potential was reversed to complete the cycle test. Three samples were tested in each group to ensure reproducibility.

To examine the bacterial growth rate and the dissolved oxygen (DO) concentration, a 1.5 mL bacteria suspension (10^8 Cells/mL) was added to 150 mL of medium and cultured at 30 °C in a shaker at 120 rpm. The DO concentration was measured using a logging DO meter (HANNA instruments HI2400, Limena, Italy). Optical density measurements were performed at different time points at 600 nm using a spectrophotometer (SpectraMAX 190, Molecular Devices™, San Jose, CA, USA).

3. Results and Discussion

3.1. Surface Morphology and Bacterial Adhesion

In order to obtain the identical surface roughness of the steel in this study, the surfaces of the 304 SS were polished to a mirror finish, since surface topography is an important factor affecting the bacterial attachment to surfaces prior to biofilm formation [29,30]. Previous studies have shown that the colonization of microorganisms on surfaces nucleates on surface irregularities and grows from these areas [31,32]. Figure 1 shows CLSM images of bacterial biofilm formed on the smooth 304 SS surfaces after the different immersion periods. They show the coverage (Figure 1a) and thickness (Figure 1b) of the *Bacillus sp.* biofilms. From the images, it can be seen that biofilm thickness increased over time, and a uniform distribution of the bacterial cells on the smooth surface was observed. Paramonova et al. found that, for microorganism biofilms less than 120 μm thick, the CLSM method reliably measures the biofilm thickness [33].

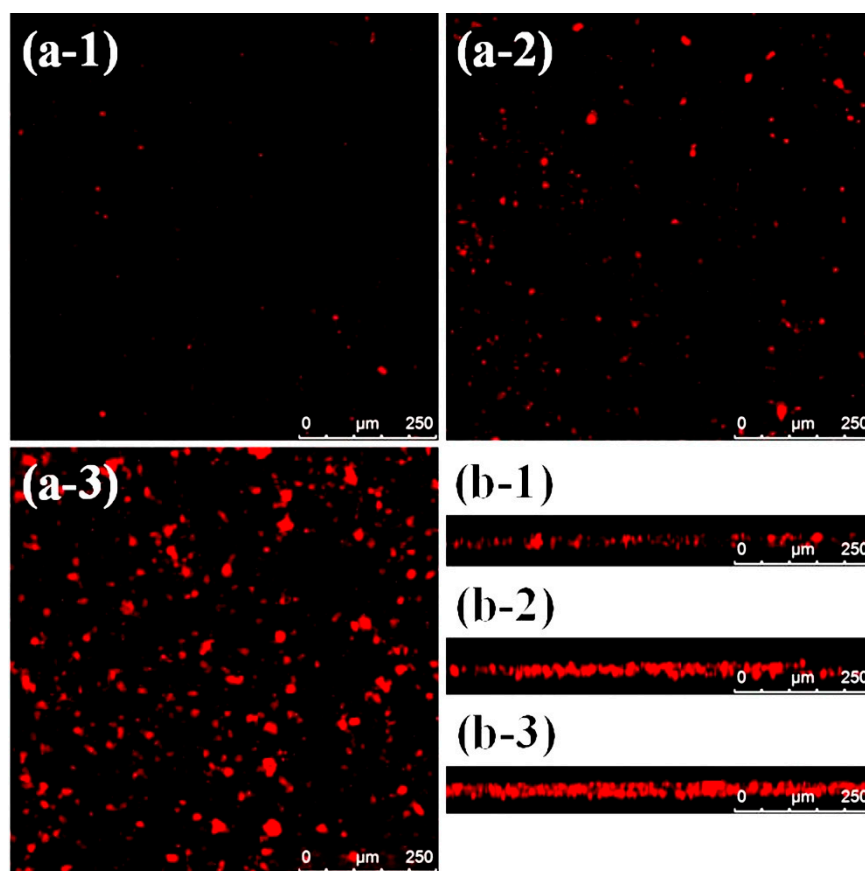


Figure 1. CLSM images of *Bacillus sp.* biofilm formed on the steel surfaces after (a-1) 1 day, (a-2) 1 week, and (a-3) 1 month and side view images of biofilm that show biofilm thickness after (b-1) 1 day, (b-2) 1 week, and (b-3) 1 month.

The topographies of the smooth surfaces in the presence and absence of biofilms are shown in Figure 2. The 304 SS average surface roughness (R_a) before and after the attachment of the bacteria were 0.58 μm (Figure 2a) and 6.30 μm (Figure 2b), respectively. These results show that the surface roughness increased significantly after the biofilm formation on the smooth surface.

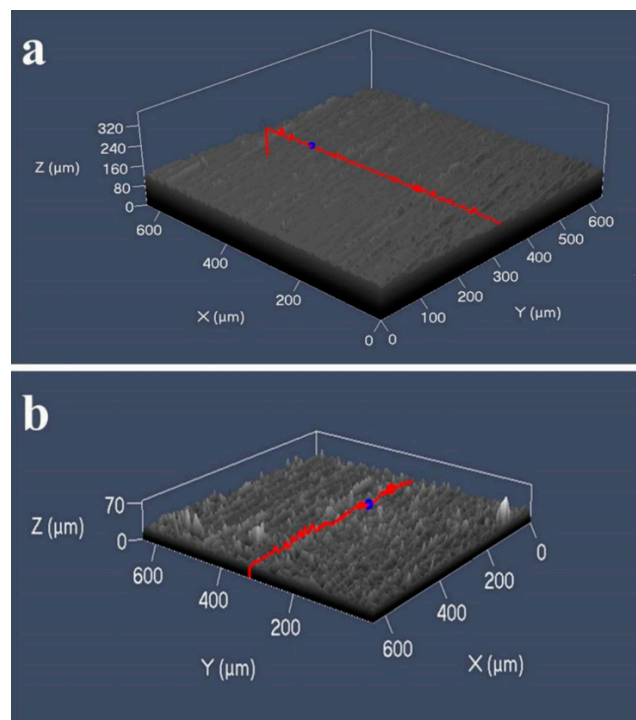


Figure 2. Surface topography of the steel plates (a) with and (b) without *Bacillus sp.* biofilm formation.

Bacterial adhesion may be significantly affected by the pH of the solution in which the steel substrates are immersed. As shown in Figure 3a, there were only a few bacteria that adhered to the substrate at a pH of 4.5, and few bacteria were observed on the substrate at a pH of 7; however, there was a dense accumulation and adhesion of the bacteria on the substrate at a pH of 9. These results suggest that the change in bacterial adhesion at different pHs was likely due to the ionization of the functional groups of *Bacillus sp.*, such as carboxyl and amino groups [34]. The electrostatic forces between the *Bacillus sp.* and the 304 SS surface were relatively weak at pH 4.5. At a pH of 7, the appearance of negatively charged carboxyl groups increased the electrostatic force of attraction between 304 SS and *Bacillus sp.*, resulting in greater adhesion. The adhesion increased further at a pH of 9 compared to that at a pH of 7 (Figure 3(a–3)). In this study, except for pH, it was also found that the temperature of the culture solution affects the bacterial adhesion. In different seasons and regions, the temperature of seawater varies greatly, generally varying from -1 to 30 °C [35]. To optimize the culture temperature for bacterial adhesion, this study has conducted bacterial adhesion tests at different temperatures. From Figure 3b, it is observed that *Bacillus sp.* produced a biofilm that contained only sparse clusters of cells at 4 °C (Figure 3(b–1)). This was probably due to the lower growth rate of the bacteria under low temperatures. However, at both 20 and 30 °C (Figure 3(b–2,b–3)), the biofilm showed a relatively complex 3D structure, consisting of dense aggregates of *Bacillus sp.* held together by an extracellular matrix. Thus, the temperature of 30 °C was chosen for the following *Bacillus sp.*-induced pitting corrosion experiments.

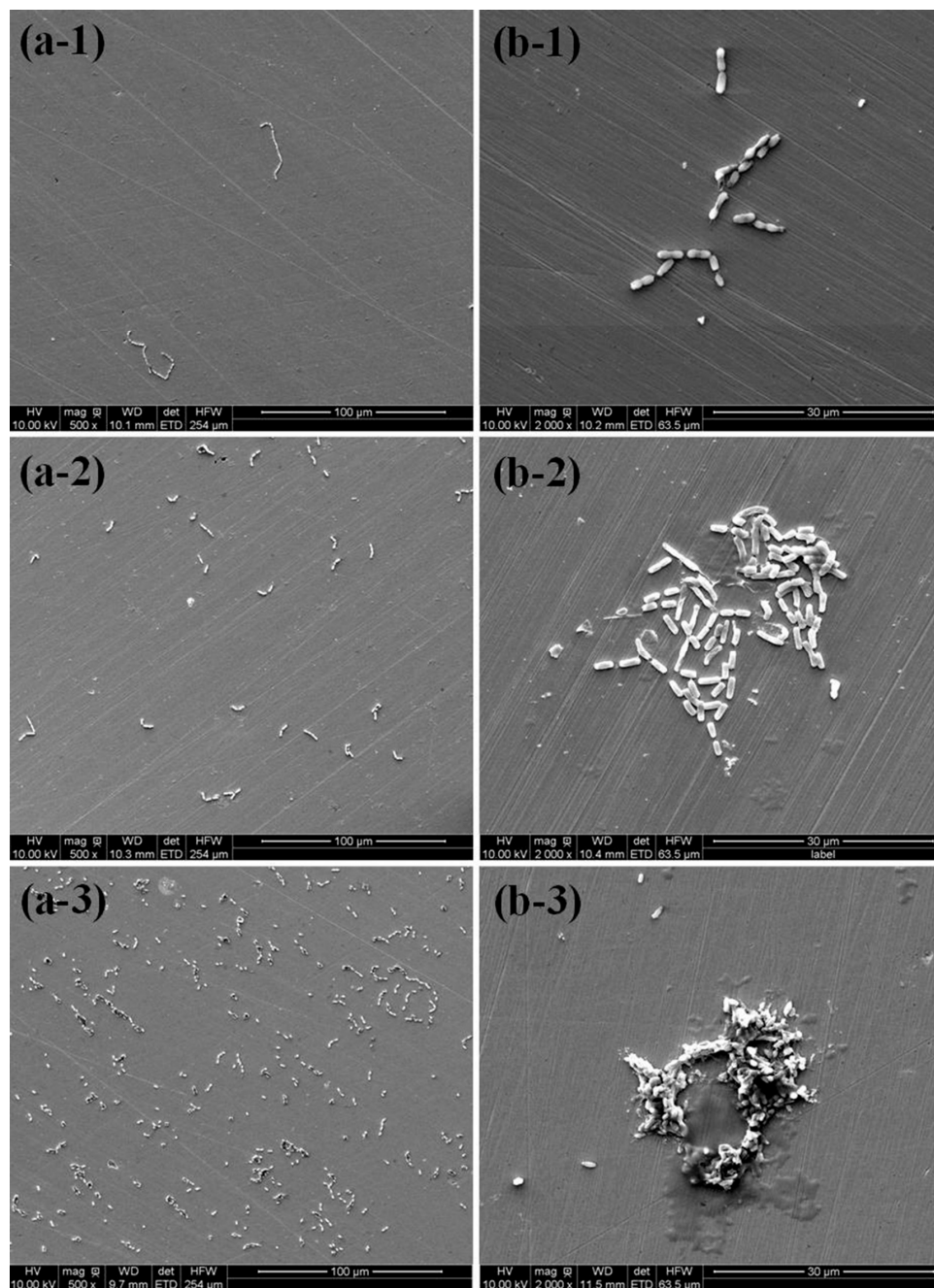


Figure 3. SEM images of the attached *Bacillus sp.* in different (a) pHs and (b) at different temperatures on the steel surface: (a-1) pH = 4.5, (a-2) pH = 7, and (a-3) pH = 9; (b-1) at 4 °C, (b-2) 20 °C, and (b-3) 30 °C.

3.2. Electrochemical Analysis

The Nyquist plots for the corrosion of the 304 SS with and without exposure to *Bacillus sp.* during the study after 90 days of immersion are shown in Figure 4a. In the presence of bacteria, the charge transfer resistance (R_{ct}) value was 212.5 k Ω ·cm², compared to that of the control in clean ASW of 7355 k Ω ·cm² after 90 days. From a previous study [28], the R_{ct} values were 1246 and 2195 k Ω ·cm² after 7 and 30 days of immersion, compared to those of the control in clean ASW of 3733 and 6908 k Ω ·cm². By comparing the R_{ct} data of 316 SS, interestingly, in the presence of bacteria, the R_{ct} of 304 SS increased first and then greatly decreased. The R_{ct} increased in the presence of bacteria after 30 days of exposure because biofilm formed on the metal surface. This was likely due to the fact that the biofilms interrupted

the flow of ions and oxygen and the biofilm acted as a protective coating to prevent corrosion. However, extended soaking for up to 90 days greatly reduced the R_{ct} to $212.5 \text{ k}\Omega\text{-cm}^2$, which was only about one tenth of that of the sample after 30 days exposure. The result indicates that the oxide film of 304 SS was greatly destroyed, and the bacteria accelerated the corrosion of stainless steel. This could have been due to the biofilm preventing oxygen from diffusing to the surface of stainless steel, causing internal and external differences in the oxygen concentration and thereby forming an oxygen concentration battery, which accelerated the corrosion of stainless steel. Therefore, the R_{ct} value decreased after 90 days of exposure. However, in clean ASW solution (control), the R_{ct} value increased with the increasing exposure time, since thin oxide layers were formed by passivation on the 304 SS surface, and these oxide layers protect alloys from aggressive media such as chlorides. In the inoculated solution, the decrease in resistance, R_{ct} , indicates that the oxide film on the surfaces is not stable in the presence of *Bacillus sp.* bacteria. This was likely due to bacteria destroying the passivation film and accelerating the pitting of stainless steel in sensitized areas, such as at grain boundaries where elements such as chromium (Cr) were dissolved and consumed, eventually causing stainless steel to fail [36]. This failure is also expected, since 304 SS alloys are vulnerable to pitting in seawater that contains *Bacillus sp.* Therefore, the weakness of the passive film at Cr-depleted regions renders the passive film in such regions less effective at protecting the underlying steel substrate and results in film breakdown and the initiation of localized corrosion [37]. In this study, to further investigate the effect of *Bacillus sp.* adhesion on the pitting corrosion of 304 SS by, the immersion time was extended to 90 days and cyclic polarization was also used to determine the change in the corrosion and pitting mechanism of the metal surface in the presence of *Bacillus sp.* (Figure 4b). It has been suggested that the tendency toward pitting may be determined by the feature of the hysteresis loop [38]. In the absence of *Bacillus sp.*, 304 SS has noticeable negative hysteresis, which suggests that pitting corrosion is not likely to occur. However, the positive hysteresis in the presence of bacteria indicates that 304 SS surfaces are susceptible to pitting (Figure 4b).

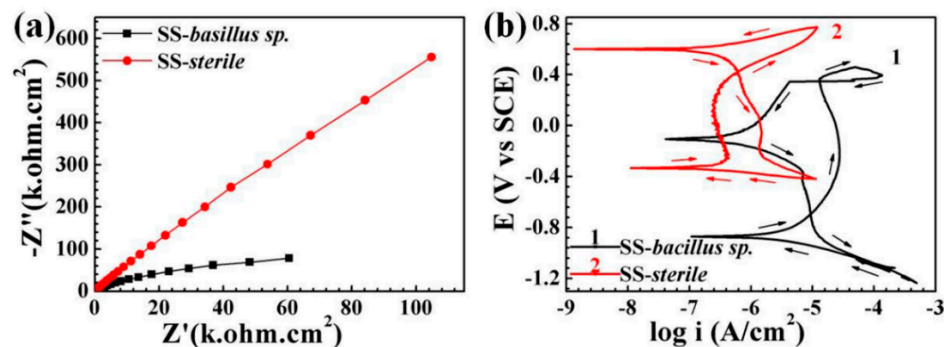


Figure 4. (a) Nyquist plots and (b) potentiodynamic polarization curves of the steel samples tested in the ASW with (*Bacillus sp.*) and without (sterile) the bacteria after 90 days of exposure. SS: the steel plates.

To understand better the effect of *Bacillus sp.* biofilm formation on the corrosion behavior of 304 SS, the dissolved oxygen (DO_2) in the solution that contained bacteria was investigated. Figure 5 shows the variation in the DO_2 concentration and *Bacillus sp.* growth during 6 h of incubation. The concentration of bacteria in the solution increased with time. The dissolved oxygen was consumed by *Bacillus sp.* and the O_2 concentration decreased to its lowest value (0.03 mg/L) after approximately 600 min of exposure. Biofilm inhibits oxygen diffusion towards the metallic surface [39], decreasing the cathodic reaction, and it will cause an inhibition of corrosion initially. It was reported that the bacteria tend to inhibit the corrosion of stainless steel in a short period [28]. However, as the exposure time was extended, this would form an oxygen concentration battery, resulting in the accelerated corrosion of stainless steel.

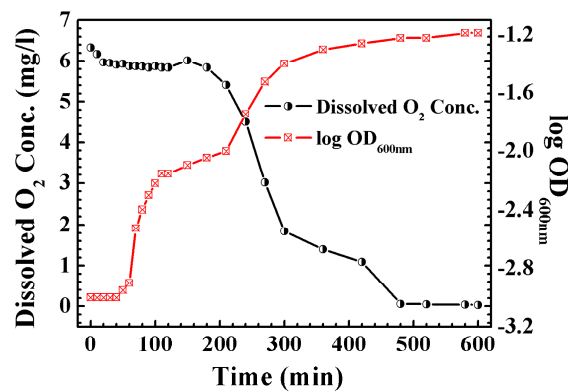


Figure 5. The variation in the dissolved oxygen concentration (mg/L) and OD_{600nm} (the absorbance of bacterial solution at 600 nm) (as a growth rate) in the bacterial solution versus time at 30 °C and 120 rpm speed. During the first 600 min of incubation, the oxygen concentrations were significantly decreased and reached their lowest value at 600 min of exposure; meanwhile, the OD_{600nm} value was incrementally increased from 0.001 to 0.06 and stayed stable.

3.3. Direct Observation of Bacteria-Induced Pitting Corrosion

Although electrochemical testing can be used to examine pitting, these approaches cannot be used to study microscale pit features [21]. In this study, direct observation, including SEM and AFM, was also performed to investigate the effect of biofilm on the pitting corrosion. The SEM analysis showed that cracks and dislocations were clearly observed on the metal surface after the removal of the biofilm (Figure 6a,b).

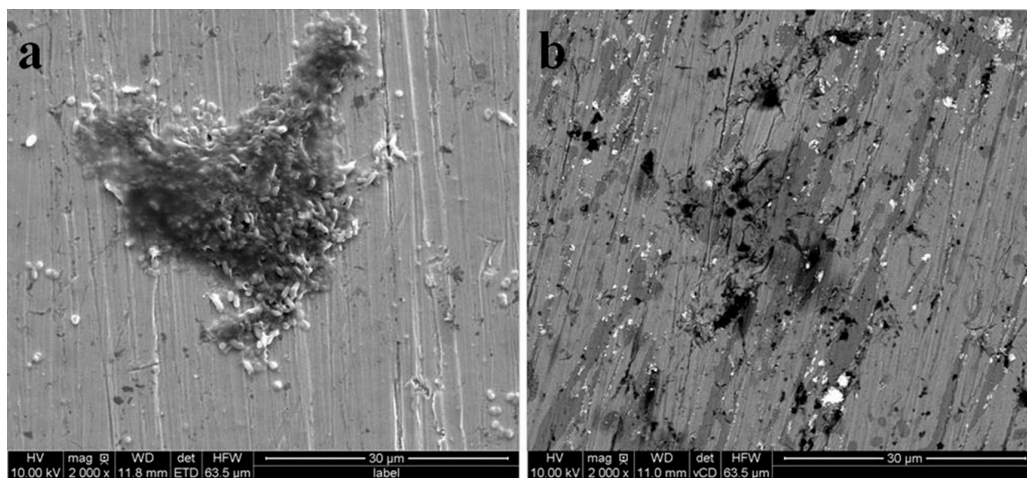


Figure 6. SEM images of the steel surfaces (a) before and (b) after removing the biofilm and corrosion by-products. These surfaces were initially exposed to artificial seawater containing *Bacillus sp.* for 90 days. Afterwards, the biofilm and corrosion by-products were removed from the surface.

To obtain detailed information of the effect of *Bacillus sp.* adhesion on the 304 SS surface, AFM observation was performed in this study. AFM images of the 304 SS exposed for 90 days to ASW that contained bacteria are shown in Figure 7. Interestingly, the AFM images before and after removing the biofilm from the 304 SS surface showed a direct correlation between the bacterial cells and underlying pits (Figure 7a,b) on the 304 SS surface. The shape and size of the pits on the steel surface are similar to those of the *Bacillus sp.* cell. This result suggests a direct role of *Bacillus sp.* on the pit initiation on the 304 SS surface. A similar result was also reported for *Desulfovibrio (D.) desulfuricans* [40].

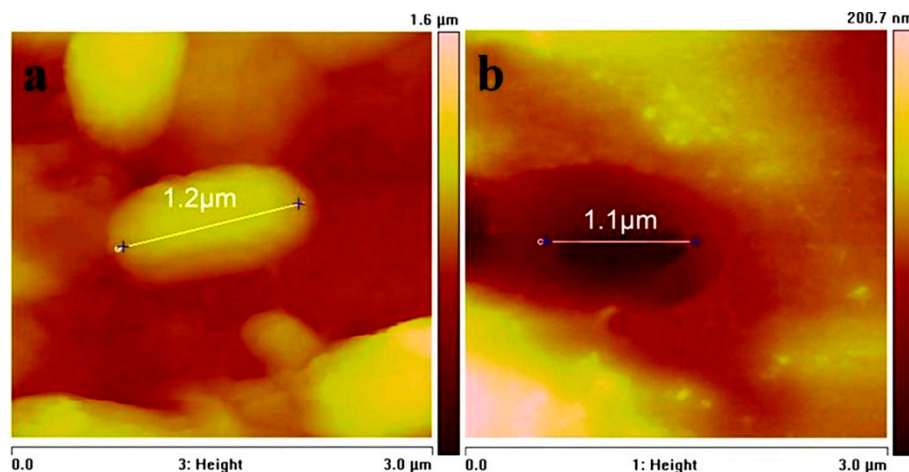


Figure 7. AFM topographical images of the steel plates after incubation for 90 days in the ASW (a) before and (b) after the removal of the biofilm that demonstrates the obvious pitting of the steel samples after the removal of the bacterial biofilm.

4. Conclusions

To simplify the study of the microbiologically induced corrosion of steel structures of high-voltage transmission line towers installed in humid environments, the attachment behaviors of a typical bacterium *Bacillus sp.* and the subsequent formation of bacterial biofilms on the steel surface were investigated. The effect of biofilm formation on the pitting corrosion of the steel surface was studied by indirect and direct methods. The adhesion of bacterium *Bacillus sp.* to the 304 SS surfaces is strongly influenced by physical and chemical parameters, including pH, temperature, and culture age. Indirect evidence from electrochemical measurements and direct evidence from SEM and AFM indicate that the adhesion of *Bacillus sp.* to metal surfaces significantly accelerated the corrosion process of 304 SS after long-term exposure (90 days) to the bacterium. Thus, the initial pitting corrosion influenced by biofilm formation can be obtained using indirect and direct methods. The results can give insight into the understanding and effective control of microbiologically induced corrosion of the steel structures of high-voltage transmission line towers.

Author Contributions: Conceptualization, J.Z. and Z.H.; methodology, J.Z. and Z.H.; software, S.H.; validation, J.Z. and Z.H.; formal analysis, J.Z., K.S., and S.H.; investigation, J.Z., K.S., S.H., and X.H.; data curation, J.Z. and K.S.; writing—original draft preparation, J.Z.; writing—review and editing, Z.H.; supervision, W.L.; project administration, Z.H.; funding acquisition, W.L. All authors have read and agreed to the published version of the manuscript.

Funding: This research was funded by China Southern Power Grid Co., Ltd. Liuzhou Bureau of EHV Transmission Company, grant number CGYKJXM2017039.

Acknowledgments: The authors acknowledge the Ningbo Institute of Materials Technology and Engineering, CAS for the experiment support, and especially thank Hua Li and Yi Liu for their great help.

Conflicts of Interest: The authors declare no conflict of interest.

References

1. Dang, H.; Lovell, C.R. Microbial surface colonization and biofilm development in marine environments. *Microbiol. Mol. Biol. Rev.* **2015**, *80*, 91–138. [[CrossRef](#)]
2. Jeffery, B.; Peppler, M.; Lima, R.S.; McDonald, A. Bactericidal effects of HOVF-sprayed nanostructured TiO₂ on pseudomonas aeruginosa. *J. Spray Technol.* **2009**, *19*, 344–349. [[CrossRef](#)]
3. George, N.; Mahon, M.; McDonald, A. Bactericidal performance of flame-sprayed nanostructured titania-copper composite coatings. *J. Spray Technol.* **2010**, *19*, 1042–1053. [[CrossRef](#)]
4. Callow, J.A.; Callow, M.E. Trends in the development of environmentally friendly fouling-resistant marine coatings. *Nat. Commun.* **2011**, *2*, 244. [[CrossRef](#)] [[PubMed](#)]

5. Posadas, E.; Garcia-Encina, P.; Soltau, A.; Dominguez, A.; Diaz, I.; Munoz, R. Carbon and nutrient removal from centrates and domestic wastewater using algal-bacterial biofilm bioreactors. *Bioresour. Technol.* **2013**, *139*, 50–58. [[CrossRef](#)] [[PubMed](#)]
6. Chambers, L.D.; Stokes, K.R.; Walsh, F.C.; Wood, R.J.K. Modern approaches to marine antifouling coatings. *Surf. Coat. Tech.* **2006**, *201*, 3642–3652. [[CrossRef](#)]
7. Gottenbos, B.; Mei, H.C.; Busscher, H.J. Initial adhesion and surface growth of staphylococcus epidermidis and pseudomonas aeruginosa on biomedical polymers. *J. Biomed. Mater. Res.* **2000**, *50*, 208–214. [[CrossRef](#)]
8. Chatterjee, S.; Biswas, N.; Datta, A.; Dey, R.; Maiti, P. Atomic force microscopy in biofilm study. *Microscopy* **2014**, *63*, 269–278. [[CrossRef](#)] [[PubMed](#)]
9. Hirai, N.; Mun, M.K.; Masuda, T.; Itoh, H.; Kanematsu, H. Atomic force MICROSCOPY-JPN analysis of biofilms formed on different plastics. *Mater. Technol.* **2014**, *30*, B57–B60. [[CrossRef](#)]
10. Cheng, C.; Zhang, Z.; Li, R.; Zhang, L.; Zhang, D.J.; Cao, T.; Min, X.; Zhao, J. Effect of temperature on pitting corrosion of 430 stainless steel under dry and wet cycle of droplet. *Surf. Technol.* **2019**, *48*, 245–251.
11. Huang, K.; McLandsborough, L.A.; Goddard, J.M. Adhesion and removal kinetics of bacillus cereus biofilms on Ni-PTFE modified stainless steel. *Biofouling* **2016**, *32*, 523–533. [[CrossRef](#)] [[PubMed](#)]
12. Yuan, S.J.; Pehkonen, S.O. Microbiologically influenced corrosion of 304 stainless steel by aerobic pseudomonas NCIMB 2021 bacteria: AFM and XPS study. *Colloids Surf. B* **2007**, *59*, 87–99. [[CrossRef](#)] [[PubMed](#)]
13. Bhandari, J.; Khan, F.; Abbassi, R.; Garaniya, V.; Ojeda, R. Modelling of pitting corrosion in marine and offshore steel structure—A technical review. *J. Loss Prev. Proc.* **2015**, *37*, 39–62. [[CrossRef](#)]
14. Krishna, N.G.; Thinaharan, C.; George, R.P.; Parvathavarthini, N.; Mudali, U.K. Surface modification of type 304 stainless steel with duplex coatings for corrosion resistance in sea water environments. *Surf. Eng.* **2014**, *31*, 39–47. [[CrossRef](#)]
15. Antony, P.J.; Chongdar, S.; Kumar, P.; Raman, R. Corrosion of 2205 duplex stainless steel in chloride medium containing sulfate-reducing bacteria. *Electrochim. Acta* **2007**, *52*, 3985–3994. [[CrossRef](#)]
16. Cheng, S.; Tian, J.; Chen, S.; Lei, Y.; Chang, X.; Liu, T.; Yin, Y. Microbially influenced corrosion of stainless steel by marine bacterium vibronatriegens: (I) Corrosion behavior. *Mat. Sci. Eng. C* **2009**, *29*, 751–755. [[CrossRef](#)]
17. Yin, Y.; Cheng, S.; Chen, S.; Tian, J.; Liu, T.; Chang, X. Microbially influenced corrosion of 303 stainless steel by marine bacterium vibronatriegens: (II) Corrosion mechanism. *Mat. Sci. Eng. C* **2009**, *29*, 756–760. [[CrossRef](#)]
18. Xu, D.; Xia, J.; Zhou, E.; Zhang, D.; Li, H.; Yang, C.; Li, Q.; Lin, H.; Li, X.; Yang, K. Accelerated corrosion of 2205 duplex stainless steel caused by marine aerobic pseudomonas aeruginosa biofilm. *Bioelectrochemistry* **2017**, *113*, 1–8. [[CrossRef](#)]
19. Rizzo, F.; Di, L.G.; Formisano, A.; Landolfo, R.A. time-dependent corrosion wastage model for wrought iron structures. *J. Mater. Civ. Eng.* **2019**, *31*, 04019165. [[CrossRef](#)]
20. Munoz, A.I.; Anton, J.G.; Guinon, J.L.; Herranz, P. Inhibition effect of chromate on the passivation and pitting corrosion of a duplex stainless steel in LiBr solutions using electrochemical techniques. *Corros. Sci.* **2007**, *49*, 3200–3225. [[CrossRef](#)]
21. Guo, P.; Plante, E.C.; Wang, B.; Chen, X.; Balonis, M.; Bauchy, M.; Sant, G. Direct observation of pitting corrosion evolutions on carbon steel surfaces at the nano-to-micro-scales. *Sci. Rep. UK* **2018**, *8*, 7990. [[CrossRef](#)] [[PubMed](#)]
22. Zhu, D.; Ooij, W.J. Corrosion protection of AA 2024-T3 by bis-[3-(triethoxysilyl)propyl]tetrasulfide in sodium chloride solution: Part 2: Mechanism for corrosion protection. *Corros. Sci.* **2003**, *45*, 2177–2197. [[CrossRef](#)]
23. Pidaparti, R.M.; Aghazadeh, B.S.; Whitfield, A.; Rao, A.S.; Mercier, G.P. Classification of corrosion defects in NiAl bronze through image analysis. *Corros. Sci.* **2010**, *52*, 3661–3666. [[CrossRef](#)]
24. Pan, C.; Liu, L.; Li, Y.; Wang, F. Pitting corrosion of 304ss nanocrystalline thin film. *Corros. Sci.* **2013**, *73*, 32–43. [[CrossRef](#)]
25. Zhang, Q.; Wang, R.; Kato, M.; Nakasa, K. Observation by atomic force microscope of corrosion product during pitting corrosion on SUS304 stainless steel. *Scr. Mater.* **2005**, *52*, 227–230. [[CrossRef](#)]
26. Abdolahi, A.; Hamzah, E.; Ibrahim, Z.; Hashim, S. Microbially influenced corrosion of steels by pseudomonas aeruginosa. *Corros. Rev.* **2014**, *32*, 129–141. [[CrossRef](#)]
27. Li, S.; Zhang, Y.; Liu, J.; Yu, M. Influence of thiobacillus ferrooxidans biofilm on the corrosion behavior of steel A3. *Int. J. Mod. Phys. B* **2010**, *24*, 3083–3088. [[CrossRef](#)]
28. Abdoli, L.; Suo, X.; Li, H. Distinctive colonization of *Bacillus sp.* bacteria and the influence of the bacterial biofilm on electrochemical behaviors of aluminum coatings. *Colloids Surf. B* **2010**, *145*, 688–694. [[CrossRef](#)]

29. Hasan, J.; Jain, S.; Radmarajan, R.; Purighalla, S.; Sambandamurthy, V.K.; Chatterjee, K. Multi-scale surface topography to minimize adherence and viability of nosocomial drug-resistant bacteria. *Mater. Des.* **2018**, *140*, 332–344. [[CrossRef](#)]
30. Liu, L.; Ercan, B.; Sun, L.; Ziemer, K.S.; Webster, T.J. Understanding the role of polymer surface nanoscale topography on inhibiting bacteria adhesion and growth. *ACS Biomater. Sci. Eng.* **2016**, *2*, 122–130. [[CrossRef](#)]
31. Pereira, M.A.; Alves, M.M.; Azeredo, J.; Mota, M.; Oliveira, R. Influence of physico-chemical properties of porous microcarriers on the adhesion of an anaerobic consortium. *J. Ind. Microbiol. Biotechnol.* **2000**, *23*, 181–186. [[CrossRef](#)]
32. Wassmann, T.; Kreis, S.; Behr, M.; Bueggers, R. The influence of surface texture and wettability on initial bacterial adhesion on titanium and zirconium oxide dental implants. *Int. J. Implant. Dent.* **2017**, *3*, 3642–3652. [[CrossRef](#)] [[PubMed](#)]
33. Paramonova, E.; Jong, E.D.; Krom, B.P.; Mei, H.C.; Busscher, H.J.; Sharma, P.K. Low-load compression testing: A novel way of measuring biofilm thickness. *Appl. Environ. Microb.* **2007**, *73*, 7023–7028. [[CrossRef](#)] [[PubMed](#)]
34. Li, X.; Ding, C.; Liao, J.; Lan, T.; Li, F.; Zhang, D.; Yang, J.; Yang, Y.; Luo, S.; Tang, J.; et al. Biosorption of uranium on *Bacillus sp.* dwc-2: Preliminary investigation on mechanism. *J. Environ. Radioact.* **2014**, *135*, 6–12. [[CrossRef](#)] [[PubMed](#)]
35. Hansen, J.; Sato, M.; Ruedy, R.; Lo, K.; Lea, D.W.; Elizade, M. Global temperature change. *Proc. Natl. Acad. Sci. USA* **2006**, *103*, 14288–14293. [[CrossRef](#)]
36. Shi, X.; Avci, R.; Geiser, M.; Lewandowski, Z. Comparative study in chemistry of microbially and electrochemically induced pitting of 316L stainless steel. *Corros. Sci.* **2003**, *45*, 2577–2595. [[CrossRef](#)]
37. Han, D.; Jiang, Y.; Shi, C.; Deng, B.; Li, J. Effect of temperature, chloride ion and pH on the crevice corrosion behavior of SAF 2205 duplex stainless steel in chloride solutions. *J. Mater. Sci.* **2012**, *47*, 1018–1025. [[CrossRef](#)]
38. Deberry, D.W.; Peyton, G.R.; Clark, W.S. Evaluation of corrosion inhibitors in SO₂ scrubber solutions. *Corrosion* **1984**, *40*, 250–256. [[CrossRef](#)]
39. Lin, J.; Ballim, R. Biocorrosion control: Current strategies and promising alternatives. *Afr. J. Biotechnol.* **2012**, *11*, 15736–15747. [[CrossRef](#)]
40. Sheng, X.; Ting, Y.; Pehkonen, S.O. The influence of sulphate-reducing bacteria biofilm on the corrosion of stainless steel AISI 316. *Corros. Sci.* **2007**, *49*, 2159–2176. [[CrossRef](#)]

Publisher's Note: MDPI stays neutral with regard to jurisdictional claims in published maps and institutional affiliations.



© 2020 by the authors. Licensee MDPI, Basel, Switzerland. This article is an open access article distributed under the terms and conditions of the Creative Commons Attribution (CC BY) license (<http://creativecommons.org/licenses/by/4.0/>).